Synthesis of Dyed Monodisperse Poly(methyl methacrylate) Colloids for the Preparation of Submicron Periodic Light-Absorbing Arrays

Albert S. Tse, Zhijun Wu, and Sanford A. Asher*

Department of Chemistry, University of Pittsburgh, Pittsburgh, Pennsylvania 15260

Received March 3, 1995; Revised Manuscript Received June 20, 1995[⊗]

ABSTRACT: We have developed a method to synthesize highly charged, monodisperse ca. 100 nm poly(methyl methacrylate) (PMMA) colloidal particles containing covalently linked absorbing dyes. We acylate these dyes with methacryloyl chloride and add these functionalized dyes during an oil-in-water emulsion polymerization of the PMMA colloids. The high charge was obtained by copolymerizing with the ionic sulfonated surfactant COPS-1. After purification these monodisperse colloids spontaneously self-assemble into crystalline colloidal arrays (CCA). We utilize this colloid to fabricate an ordered array of absorbing colloidal spheres locked into a hydrogel matrix. We exchange the water in the medium to approximately match the real part of the array refractive index. This forms a novel submicron periodic system where a body-centered cubic array of absorbers interact with electromagnetic radiation with little scattering or diffraction of the incident light.

Introduction

Monodisperse colloidal particles have many applications in numerous areas of technology and the physical and biomedical sciences. They are used as calibration standards for electron microscopy, as model systems in light scattering and small-angle neutron scattering, and for studies of rheology of dispersions and aerosol research. Monodisperse latex particles have also been extensively employed in various diagnostic tests, in vitro immunoassays, bone marrow transplantations, drug delivery systems, flow cytometry standards, and media for cell and protein separations.[1-3]

Numerous synthetic methods have been described to prepare monodisperse charged particles of organic polymers such as polystyrene[4-7] and poly(methyl methacrylate) (PMMA)[8-10] and inorganic colloids such as silica.[11,12] Numerous other approaches exist to form monodisperse colloids of unique shapes for a variety of applications.[13]

Our interest in monodisperse colloidal particles is centered on using their novel self-assembly processes to form crystalline colloidal arrays (CCA) which Bragg diffract light.[14-18] Highly charged monodisperse colloids strongly electrostatically repel one another when their spacings occur within a Debye layer length (<1 μm). Concentrated colloidal dispersions (>10^{13} particles/mL) in deionized water show interaction potentials greater than kT, where k is the Boltzmann constant and T is the temperature; the lowest energy state of the system is where the particles self-assemble into a CCA which is in a body-centered cubic (bcc) or face-centered cubic (fcc) crystal structure. The spacing of the array is comparable to visible and near-IR light and, thus, strong Bragg diffraction occurs from the arrays. We have utilized these CCA as Bragg diffraction filters for spectroscopic applications.[19,20]

We have proposed that these CCA can be used for optical switching and optical limiting applications. The idea is to match the real part of the refractive index of nonlinear colloidal particles such that at normal light intensities no scattering or Bragg diffraction occurs from the array.[21,22] However, the particles in the array are synthesized to have large optical nonlinearities, and at high light intensities the refractive index of the particles diverges from that of the medium; the CCA array "pops up" to diffract the high-intensity incident light. We have calculated that refractive index differences as small as 0.01 would permit the switch to operate efficiently.

The required colloidal particle nonlinearities exceed that of most known materials. Two possible approaches exist. We can utilize the large nonlinearities of cadmium sulfide (CdS) quantum dots,[12,23] or we can use the larger nonlinear phenomena associated with thermal processes. We recently theoretically investigated the utility of using absorbing spheres to transfer energy from an intense incident beam to heat the colloidal particles to alter the particle refractive index.[21] Our calculations indicate that nanosecond switching should occur for incident powers of 10 MW/cm^2.

In the work here we describe a general method to synthesize highly charged, monodisperse ca. 100 nm poly(methyl methacrylate) (PMMA) colloidal particles containing covalently linked absorbing, nonfluorescent dyes. This work follows our earlier studies of polystyrene colloids physically mixed with the disazo dye Oil Red O to study photothermal compression,[24] thermal diffuse scattering,[25] and collective diffusion[26] of CCA. However, the nonlinear application requires a covalent dye linkage because the nonlinear colloids are in a more hydrophobic medium than water, where physisorbed dyes are soluble and would partition out of the spheres into the medium.

Other examples have been reported for covalent attachment of dyes to monodisperse particles. For example, Bhattacharyya and Halpern[2] reported the covalent attachment of fluorescent moieties to monodisperse latex particles without providing experimental details. Winnik and co-workers[27] prepared fluorescent-labeled PMMA latexes by semicontinuous emulsion polymerization. These dyes possessed either vinyl or methacryloyl groups. Peterson[28] was issued a patent for the process of copolymerizing acrylamide with a pH-indicating dye such as Phenol Red to form a macroscopic hydrophilic copolymer. Lyophilized polystyrene spheres were then mechanically mixed with the dried dyed

* To whom correspondence should be addressed.
[⊗] Abstract published in *Advance ACS Abstracts,* August 1, 1995.

0024-9297/95/2228-6533$09.00/0

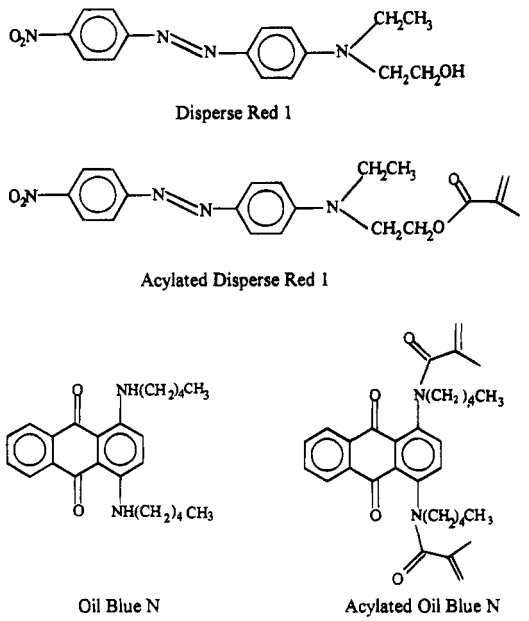

Figure 1. Structures of Disperse Red 1 and Oil Blue N before and after methacryloyl chloride acylation.

Table 1. Recipe for Emulsion Polymerization of Dyed PMMA Colloid

first stage	
water	233 mL
MMA	12.00 g
DVB	1.12 g
COPS-1	0.927 g
SDS	0.057–0.150 g
$Na_2S_2O_8$	0.120 g
second stage	
MMA	35.90 g
DVB	3.35 g
Acylated Dye	0.075–1.750 g

polyacrylamide spheres to fabricate fiber optic pH probes.

Experimental Section

The dyes 4-[ethyl(2-hydroxyethyl)amino]-4′-nitroazobenzene (Disperse Red 1, Colour Index (CI) 11110), and 1,4-bis(pentylamino)-9,10-anthraquinone (Oil Blue N, CI 61555) were obtained from Aldrich Chemical Co. and used as received (Figure 1). The dye acylation procedure followed that of Loucif-Saïbi et al.[29] A mixture of 0.30 g of dye, 5 mL of triethylamine (Mallinckrodt), and 5 mL of dry THF was cooled to 0 °C, and 0.23 g of distilled methacryloyl chloride (Aldrich) was added dropwise while stirring. The mixture was stirred for 2 h at 0 °C and then at room temperature for 16 h. The product was washed with excess distilled water, filtered, and dried at room temperature in vacuo. Successful acylation was confirmed by thin-layer chromatography, NMR, and UV–visible spectroscopies. The structures of the dyes before and after acylation are shown in Figure 1.

The two-stage PMMA emulsion polymerization reaction was modified from the procedure of Brnardic[30] and Wolfe and Scopazzi.[10] Table 1 shows a typical recipe. In the first stage, 225 mL of deionized water (Barnstead Nanopure water purification system) and sodium dodecyl sulfate (SDS, Sigma Chemical) detergent were added to a 500 mL reaction kettle (Ace Glass) equipped with a mechanical stirrer, reflux condenser, nitrogen inlet, and thermometer. The kettle was placed in a heating mantle which was connected to a temperature controller (Ace Glass, Model 12106). The stirred mixture was thermostated at 83 ± 2 °C and bubbled with nitrogen at a low rate for 60 min. The nitrogen tube was lifted above the reaction mixture and a low rate of gas flow was maintained during the reaction. Methyl methacrylate (MMA) and divinylbenzene (DVB) (both from Aldrich) were deinhibited by a column of activated aluminum oxide (Aldrich). A mixture of 12.00 g of MMA and 1.12 g of DVB was injected over a 30 min period via a syringe pump. The ionic comonomer sodium 1-(allyloxy)-2-hydroxypropanesulfonate (COPS-1) (CH_2=$CHCH_2OCH_2CH(OH)CH_2SO_3^-Na^+$) in 40% aqueous solution was obtained from Rhône-Poulenc and was used as supplied. COPS-1 (0.927 g) diluted with 5 mL of water was simultaneously injected by using a separate syringe pump. The sodium persulfate initiator (Aldrich) was dissolved in 3 mL of water and added after the first-stage monomer addition was complete. When the polymerization began, the temperature rose from 83 to 88 °C and dropped to 83 °C after 15 min. After 40 min of polymerization, a mixture of 35.90 g of MMA and 3.35 g of DVB containing the acylated dye was injected over a period of 60 min. The reaction was continued for 1 h and 50 min to ensure complete reaction of the monomers for a total reaction time of 3.5 h.

The polymerization was followed by removing ca. 2 mL of sample from the kettle at different time intervals to determine the percent conversion, particle size, and size distribution. Hydroquinone (Fisher Scientific) was used to stop the polymerization. An aliquot was dried in the presence of ca. 1% hydroquinone in an oven at 105 °C for 2 h to determine the degree of conversion.

The reaction product was filtered through glass wool to remove any coagulum. The iridescence of the colloidal crystals could be observed even before purification by shaking the samples with ion exchange resin for 30 min. Typically, the colloidal samples were dialyzed against deionized water for 2 weeks using 50 000 molecular weight cutoff Spectra/Por 6 dialysis tubing (Fisher Scientific) with the water changed every 24 h. Subsequently, the dialyzed suspension was shaken with Bio-Rad AG 501-X8 mixed-bed ion exchange resin for 48 h using a mechanical shaker.

The particle diameter was determined by quasi-elastic light scattering (QELS) and by transmission electron microscopy (Zeiss EM 902A). QELS measurements were performed at 90° scattering angle with a Malvern Zetasizer 4. The cumulant technique was used to determine the light scattering z-average mean diameter and the index of polydispersity (Q) of the particle size distribution. In the cumulant analysis, the logarithm of the normalized correlation function is fitted by a second-order polynomial after removal of the baseline over time t

$$\log\{(G(t)/\langle N\rangle^2) - 1\} = L + Mt + Nt^2 \qquad (1)$$

where $G(t)$ is the second-order autocorrelation function, $\langle N\rangle$ is the baseline intensity, and L, M, and N are the regression coefficients of the cumulant fit. M gives the z-average mean size and Q, defined as N/M^2, measures the variance of the particle size distribution. Q is zero for monodisperse spheres and is typically 0.02–0.05 for latexes with narrow distributions.

After vigorous cleaning, the surface charge density of the dyed spheres was determined by conductometric titration with 0.01 N sodium hydroxide solution. Twelve grams of the latex sample containing ca. 6% solids was titrated, and the specific conductivity was measured by a conductance meter (YSI Model 35). The shapes of the titration curves are typical of those found in titrations of a strong acid with a strong base. The molar absorptivities were determined by dissolving the dyes in spectrophotometric grade acetonitrile (Mallinckrodt) and the transmission spectra obtained with a Perkin-Elmer Lambda 9 UV–visible–near-IR spectrophotometer.

The dye concentration in the latex was determined by UV–visible spectroscopy. To minimize the scattering from the colloidal particles, the particles were refractive index matched by adding methyl phenyl sulfoxide (MPSO) (Aldrich), which is a high refractive index (n = 1.58), water-miscible solvent. In a typical procedure, 0.10 g of dyed latex was diluted with 0.58 g of water and 2.00 g of MPSO to give a refractive index of 1.51. The refractive index of the suspension was measured by an Abbè refractometer (Bausch and Lomb) thermostated at 23 °C.

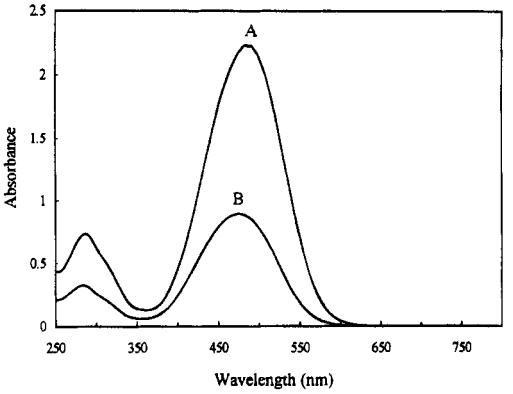

Figure 2. Absorption spectra of (A) 0.31 mM Disperse Red 1 in acetonitrile before acylation and (B) 0.13 mM dye after acylation with methacryloyl chloride. Path length = 0.2 cm.

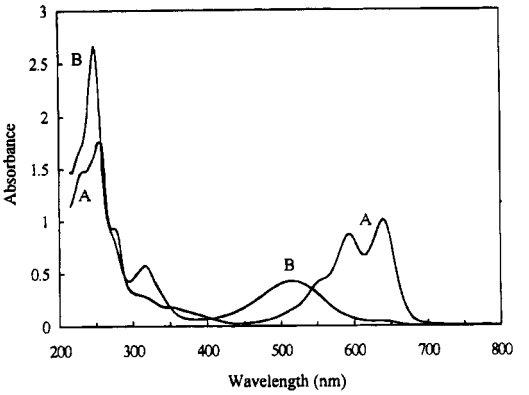

Figure 3. Absorption spectra of (A) 0.31 mM Oil Blue N in acetonitrile before acylation and (B) 0.31 mM dye after acylation with methacryloyl chloride. Path length = 0.2 cm.

We used a procedure modified from that of Asher et al.[31] to polymerize the dyed spheres within polyacrylamide hydrogels. In a typical preparation, 93.6 mg of acrylamide monomer, 14.6 mg of *N,N'*-methylenebisacrylamide cross-linker (both Fluka electrophoresis grade), 20.0 mg of *N*-vinyl-2-pyrrolidone comonomer (Aldrich), and 10.0 mg of a solution of equal volumes of 2,2-diethoxyacetophenone photoinitiator (Aldrich) and dimethyl sulfoxide (Fisher Scientific) were mixed with 1.5 mL of dyed PMMA colloid and shaken with ion exchange resin until the iridescence returned. The mixture was degassed under vacuum, injected slowly into quartz cells, and polymerized under a 365 nm UV lamp (Blak Ray B-100Y) for 4 h. The strength and porosity of the hydrogel films were controlled by varying the *N,N'*-methylenebisacrylamide and *N*-vinyl-2-pyrrolidone concentrations. The volume fraction of PMMA colloid in the particle–hydrogel composite was estimated to be 7%.

Results and Discussion

Acylation of Dyes. Since no oil-soluble, nonfluorescent dyes with polymerizable vinyl groups are commercially available, we introduce vinyl groups into the dyes by acylation using methacryloyl chloride. The azo dye Disperse Red 1 was chosen for acylation because it absorbs in the yellow/orange/red areas. The UV–visible spectra of Disperse Red 1 in acetonitrile before and after acylation (Figure 2) show that acylation of the terminal OH group results in blue shifts of the 485 and 287 nm bands to 474 and 283 nm, respectively. The molar absorptivities remained essentially identical ($\epsilon = 3.4 \times 10^4$ M^{-1} cm^{-1} at 474 nm after acylation). NMR spectra of the acylated Disperse Red 1 showed the presence of the C=C double bond from methacryloyl chloride and aromatic rings from the dye.

We have also utilized the 1,4-disubstituted anthraquinone Oil Blue N dye, which absorbs in the 600–650 nm region and is compatible with acrylic polymers.[32] The absorption spectrum of Oil Blue N shows two peaks of similar intensities at 640 and 594 nm which may be due to an underlying Franck–Condon progression. Strong absorption also occurs for a UV band at ca. 260 nm. Acylation of the two secondary amino groups by methacryloyl chloride results in a blue shift of the visible bands to a single broad peak with a maximum at 515 nm. The absorptivity decreases by 60% while the absorbance of the UV bands increases (Figure 3). This type of wavelength shift has been reported for the acylation of substituted anthraquinone dyes with methacryloyl chloride.[33] Acylation may reduce the conjugation of the anthraquinone ring by preventing hydrogen bonding of the NH groups to the carbonyl groups and by twisting the amine out of conjugation. Table 2 shows the absorption maxima and molar absorptivities of the two dyes before and after acylation.

Table 2. Molar Absorptivities of Dyes before and after Acylation[a]

dye	λ_{max} (nm)	ϵ (M^{-1} cm^{-1})
Disperse Red 1		
before	485	3.6×10^4
	287	1.2×10^4
after	475	3.4×10^4
	283	1.3×10^4
Oil Blue N		
before	640	1.6×10^4
	594	1.4×10^4
	256	2.8×10^4
after	515	0.7×10^4
	318	0.9×10^4
	250	4.2×10^4

[a] λ_{max} = absorption wavelength maximum; ϵ = molar absorptivity.

Dyed PMMA Latexes. The first stage of the emulsion polymerization utilized 25% of the monomers and the ionic comonomer COPS-1 to generate the seed particles, while in the second stage, the remaining 75% of the monomers with the dissolved dye was continuously injected into the kettle to permit the particles to grow to the desired size. With this semicontinuous emulsion polymerization technique, we could synthesize dyed monodisperse PMMA particles with any size between 60 and 210 nm by varying the SDS concentration.

The time course of polymerization was followed for the reaction using 0.060 g of SDS and 0.105 g of acylated Disperse Red 1. For the first-stage polymerization the conversion was 72% of the amount added and the size was 122 nm within 10 min of reaction, showing that the reaction is fast. The conversion reached 91% and the size was 129 nm at the end of the first stage after 40 min. The full conversion–time curve and the size–time curve including both stages are shown in Figures 4 and 5, respectively, where the conversion percentage was normalized to the total amount of monomer added. The size at the end of the reaction was 205 nm at 99% conversion. The linearity of the conversion vs time from 50 to 100 min during the second-stage monomer addition is related to the fact that the polymerization is under a "starved" condition and the reaction rate is controlled by the rate of monomer addition. The particle growth in the second stage in terms of the particle volume was also found to be linear with time. This is taken as evidence that no new particles are generated

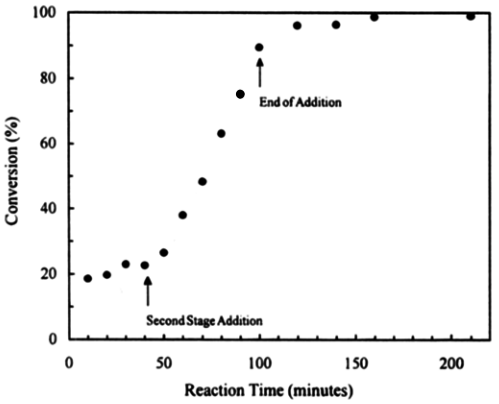

Figure 4. Conversion–time curve of emulsion polymerization of MMA with Disperse Red 1.

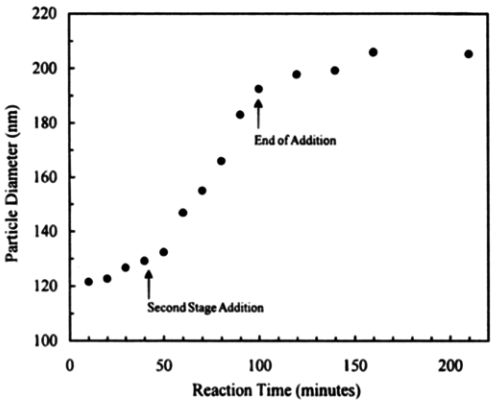

Figure 5. Size–time curve of emulsion polymerization of MMA with Disperse Red 1.

in the second stage. However, within the standard deviation of the measured particle size, it is not possible to specify whether the diameter or the (diameter)^3 is changing linearly with time.

The polydispersity index by QELS at different time intervals ranged from 0.02 to 0.07. This indicates that the particles were relatively monodisperse throughout the reaction. The particle concentration (n_p) in the suspensions was calculated from the % solids and the particle diameter (d)

$$n_p = (\%\ \text{solids}/100)(\text{latex density})/(\pi d^3 \varrho/6) \quad (2)$$

where ϱ is the density of PMMA and is 1.19 g/mL. The density of the cross-linked latex was determined to be 1.15 g/mL. The average number of particles was (3.8 $\pm$ 0.3) $\times$ 10^{13} per mL and remained constant throughout the rest of the reaction. Apparently, nucleation was complete within the first 10 min and few new nuclei formed in the second stage.

Figure 6 shows a transmission electron micrograph of PMMA colloids with Disperse Red 1 covalently attached. The particles were spherical and monodisperse with an average size of 92 $\pm$ 2 nm, which is significantly smaller than the value of 123 nm as measured by QELS. This smaller size is probably due to the partial shrinkage of the particles in the electron beam by the free radical chain depolymerization of PMMA.[9] Tables 3 and 4 list the properties of PMMA–Disperse Red 1 and PMMA–Oil Blue N colloids, respectively. The particle size ranges between 100 and 200 nm with low polydispersities. The particle number density is ca. 10^{13} per mL. The surface charges of the colloids are derived from both the sulfate groups from

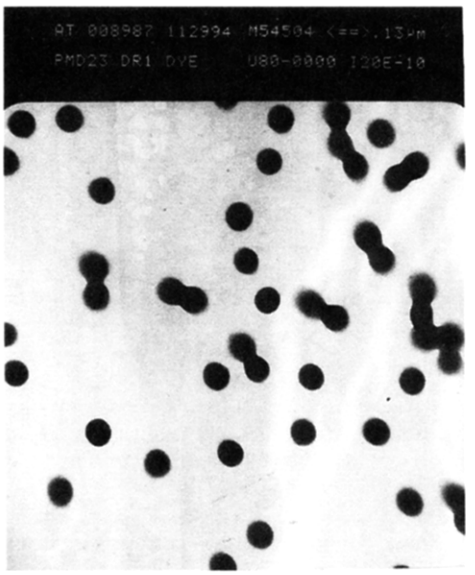

Figure 6. Transmission electron micrograph of PMMA colloids with Disperse Red 1.

the initiator and sulfonate groups from the COPS-1. The charge density of the colloids is on the order of 1.0 μC/cm^2, which is about 8000 charges per particle for a 190 nm particle size. The charge densities are comparable to those of PMMA colloids prepared with the same recipe without dye.

The dye concentration in the latex was determined by absorption measurements of the refractive index matched spheres. The refractive index of the PMMA spheres with 9.3 wt % DVB cross-linker (n = 1.57) is 1.51, which is higher than the value of 1.49 for pure PMMA. At the index-matched point of n = 1.51, no scattering from the colloid occurs, and the absorbance measured is only due to the dye absorption. Here, we assume that the molar absorptivity of the dye bound to the PMMA particles is identical to that of the acylated dye. The dye concentrations range from 0.4 to 6.5 mM or 0.071–1.2 wt % of the colloids (Tables 3 and 4). The absorption cross section (σ_a) of the dyed particles at the refractive index matched point was calculated using the equation

$$\sigma_a = A/(0.434 n_p b) \quad (3)$$

where A is the absorbance and b is the path length. The absorption cross sections of the dyed colloidal particles are all on the order of 10^{-13} cm^2. The actual cross section of a PMMA sphere without dye is of the order of 10^{-10} cm^2. Thus the absorption cross section is ca. 0.1% of the physical area of a PMMA particle.

To prove that the dye was covalently attached to the PMMA, we tried to extract the dye from the colloid. The PMMA–Disperse Red 1 colloid was dried at 105 °C for 2 h, cooled, and extracted with different organic solvents. For ethylene glycol the solvent remained colorless and the colloid red colored. There was a slight extraction by dimethyl sulfoxide and MPSO. This could be due to the presence of traces of unreacted dye. Similar results were observed for PMMA–Oil Blue N spheres. As a control, we also added Disperse Red 1 dye to the PMMA colloids. The dye partitions into the PMMA spheres but is easily extracted with organic solvents such as ethylene glycol or benzyl alcohol.

Hydrogel Crystalline Colloidal Arrays of Dyed PMMA. After removal of ionic impurities these highly charged dyed monodisperse PMMA spheres spontane-

Table 3. Properties of PMMA Colloid with Disperse Red 1[a]

% solids	d (nm)	Q	n_p (mL^{-1})	S (μC/cm^2)	c (mM)	σ_a (cm^2/part.)	σ_p (cm^2/part.)
15.9	123	0.043	16.0×10^{13}	0.9	2.2	8.3×10^{-13}	1.2×10^{-10}
10.2	141	0.043	6.8×10^{13}	1.2	6.5	58.0×10^{-13}	1.6×10^{-10}
17.6	186	0.029	5.1×10^{13}	1.0	0.4	7.1×10^{-13}	2.7×10^{-10}
17.0	205	0.032	3.7×10^{13}	0.9	1.0	4.0×10^{-13}	3.3×10^{-10}

[a] d = z-average mean diameter; Q = polydispersidty index; n_p = number density of particles; S = charge density; c = dye concentration in colloid; σ_a = particle absorption cross section; σ_p = particle cross-sectional area.

Table 4. Properties of PMMA Colloid with Oil Blue N[a]

% solids	d (nm)	Q	n_p (mL^{-1})	S (μC/cm^2)	c (mM)	σ_a (cm^2/part.)	σ_p (cm^2/part.)
10.7	131	0.014	8.9×10^{13}	1.1	2.3	4.2×10^{-13}	1.3×10^{-10}
18.5	194	0.057	4.8×10^{13}	1.0	0.7	2.5×10^{-13}	3.0×10^{-10}

[a] d = z-average mean diameter; Q = polydispersity index; n_p = number density of particles; S = charge density; c = dye concentration in colloid; σ_a = particle absorption cross section; σ_p = particle cross-sectional area.

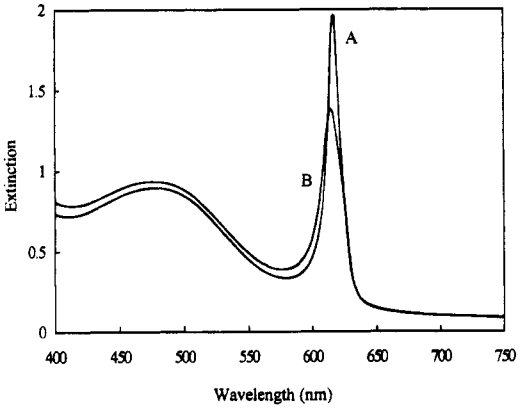

Figure 7. UV–visible spectra of (A) a 0.22 mm thick liquid CCA of PMMA–Disperse Red 1 before gelation and (B) the polymerized CCA.

ously self-assemble due to electrostatic interactions into bcc or fcc structures called crystalline colloidal arrays (CCA). Diffraction from these well-ordered CCA almost follows Bragg's law[16]

$$\lambda_0 = 2nd \sin \theta \tag{4}$$

where λ_0 is the wavelength of the light in vacuum, n is the refractive index of the system, d is the interplane spacing, and θ is the Bragg angle. In general, the extinction (E = −log{transmission}) of 0.22 mm thick CCA ranges from 1 to above 5 depending on the CCA ordering, the particle size, and the refractive index mismatch between the colloidal spheres and the medium.

Figure 7A shows the extinction spectrum of a CCA prepared from the 123 nm PMMA colloids containing Disperse Red 1. The CCA medium consists of a mainly aqueous medium which contains polymerizable monomers and the photoinitiator. The peak at 617 nm is due to the CCA Bragg diffraction while the broad peak at 475 nm is due to dye absorption. The interplane spacing d_{110} is about 204 nm and the nearest neighbor interparticle spacing is 250 nm assuming a bcc structure. The surface to surface distance of the colloidal spheres is about one particle diameter. After illumination with UV light, a hydrogel forms to lock in the CCA particle ordering.[34,35] Figure 7B shows the extinction spectrum of this polymerized CCA. The extinction of the diffracting peak decreased from 1.9 to 1.4 after gelation. There was a slight peak shift to 614 nm. The broad dye absorption peak at 478 nm was not affected by gelation. The similarities of the two diffraction peaks indicates that the lattice was little disturbed upon polymerization.

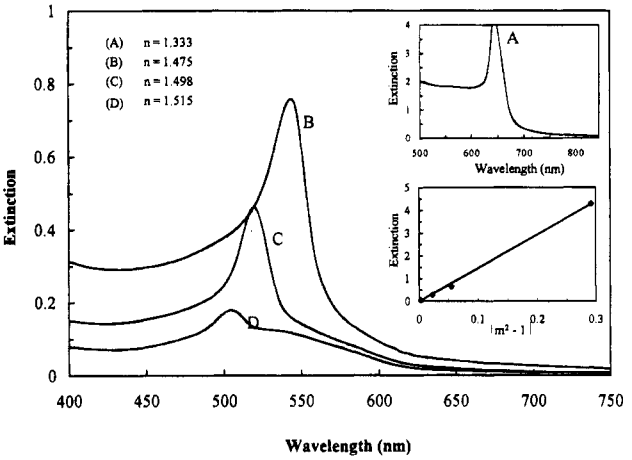

Figure 8. UV–visible spectra of 0.44 mm thick polymerized CCA of PMMA–Oil Blue N in water/MPSO solutions of different refractive indices: (A) 0 wt % MPSO; (B) 62 wt % MPSO; (C) 71 wt % MPSO; (D) 76 wt % MPSO.

The medium of the CCA hydrogel can be exchanged by adding other solvents such as MPSO to change the refractive index mismatch between the spheres and the medium. This will dramatically alter the CCA diffraction intensity since the extinction depends linearly upon the refractive index mismatch between the spheres and the medium

$$E \propto |m^2 - 1| \tag{5}$$

where $m = n_s/n_m$; n_s and n_m are the refractive indices of the spheres and the medium, respectively.[36] Figure 8 shows the spectra of a 0.44 mm thick hydrogel CCA of 184 nm PMMA colloids containing covalently linked Oil Blue N with a medium containing various concentrations of water and MPSO. For pure water, the refractive index mismatch is $\Delta n \cong 0.28$, and the extinction of the diffraction peak at 640 nm is above 4 (Figure 8A). There is a large decrease in extinction to 0.76 when the medium refractive index increases to 1.475 ($\Delta n \cong$ 0.04, Figure 8B). The peak also blue shifts to 543 nm due to the shrinkage of the hydrogel upon addition of MPSO. When the real part of the array refractive index is approximately matched with the medium at n = 1.515, the extinction maximum is 0.18 and the peak position shifts to 508 nm (Figure 8D). The underlying broad peak, which is most evident in Figure 8D, results from the absorption of acylated Oil Blue N, which has a maximum at 515 nm. The refractive index matching also results in a significant decrease in the background diffuse scattering of the CCA and the hydrogel matrix.

The inset in Figure 8 demonstrates that the diffraction extinction is proportional to $|m^2 - 1|$.

Alterations in the diffracted wavelength must result from changes in the wavelength of light in the medium. The mean refractive index is increased as the medium refractive index approaches that of the spheres. This should shift the observed peak to the red; for λ_0/n to stay constant when n increases, λ_0 must also increase. The observed diffracted wavelength blue shift results from a gel shrinkage due to the changing properties of the medium. In the case here the lattice spacing contracts. This turns out to be a useful independent method for varying the diffraction wavelength. Unfortunately, for these gels some disordering of the lattice begins to become evident as the refractive index matching condition begins to be met. This decreases the Bragg efficiency somewhat from that expected. This becomes serious at higher refractive indices where the medium refractive index becomes greater than that of the colloids. The hydrogel array appears to be either in a fcc lattice or a mixed fcc–bcc array or in a random stacked hexagonal array. The quality of the Kossel rings makes it difficult to determine the crystal structure in the refractive index matched gels.

Conclusions

We have created an ordered array of absorbers locked in a hydrogel matrix. The absorbers are contained in ca. 150 nm colloids arrayed in a lattice. The absorbers are relatively dilute within the colloidal particles to give each colloidal particle a cross section of 10^{-13} cm^2, which is almost 1000-fold smaller than that of the colloidal particle cross-sectional area. This system may be useful for nonlinear optical switching and limiting applications.

Acknowledgment. The authors gratefully acknowledge financial support from the Air Force Office of Scientific Research through Grant No. F49620-93-1-0008, Office of Naval Research through Grant No. N00014-94-1-0592, and from the University of Pittsburgh Materials Research Center through the Air Force Office of Scientific Research Grant No. AFOSR-91-0441. We thank a reviewer for pointing out the importance of hydrogen bonding in the absorption of the anthraquinone dye Oil Blue N.

References and Notes

(1) *Future Directions in Polymer Colloids*. El-Aasser, M. S., Fitch, R. M., Eds.; Martinus Nijhoff: Dordrecht, 1987.
(2) Bhattacharyya, B. R.; Halpern, B. D. *Polym. News* **1977**, *4*, 107.
(3) *Scientific Methods for the Study of Polymer Colloids and Their Applications*. Candau, F., Ottewill, R. H., Eds.; Kluwer Academic: Dordrecht, 1990.
(4) Woods, M. E.; Dodge, J. S.; Krieger, I. M. *J. Paint Technol.* **1968**, *40*, 541.
(5) Kamel, A. A.; El-Aasser, M. S.; Vanderhoff, J. W. *J. Dispersion Sci. Technol.* **1981**, *2*, 183.
(6) Tsaur, S. L.; Fitch, R. M. *J. Colloid Interface Sci.* **1987**, *115*, 450.
(7) Sunkara, H. B.; Jethmalani, J. M.; Ford, W. T. *J. Polym. Sci., Polym. Chem. Ed.* **1994**, *32*, 1431.
(8) Ono, H.; Saeki, H. *Colloid Polym. Sci.* **1975**, *253*, 744.
(9) Fitch, R. M.; Tsai, C. H. In *Polymer Colloids*; Fitch, R. M., Ed.; Plenum: New York, 1975; p 73.
(10) Wolfe, M. S.; Scopazzi, C. *J. Colloid Interface Sci.* **1989**, *133*, 265.
(11) Stöber, W.; Fink, A.; Bohn, E. *J. Colloid Interface Sci.* **1968**, *26*, 62.
(12) (a) Chang, S. Y.; Liu, L.; Asher, S. A. *J. Am. Chem. Soc.* **1994**, *116*, 6739. (b) Chang, S. Y.; Liu, L.; Asher, S. A. *J. Am. Chem. Soc.* **1994**, *116*, 6745.
(13) Matijevic, E. *Pure Appl. Chem.* **1988**, *60*, 1479.
(14) Carlson, R. J.; Asher, S. A. *Appl. Spectrosc.* **1984**, *38*, 297.
(15) Flaugh, P. L.; O'Donnell, S. E.; Asher, S. A. *Appl. Spectrosc.* **1984**, *38*, 847.
(16) Rundquist, P. A.; Photinos, P.; Jagannathan, S.; Asher, S. A. *J. Chem. Phys.* **1989**, *91*, 4932.
(17) Kesavamoorthy, R.; Jagannathan, S.; Rundquist, P. A.; Asher, S. A. *J. Chem. Phys.* **1991**, *94*, 5172.
(18) Kesavamoorthy, R.; Tandon, S.; Xu, S.; Jagannathan, S.; Asher, S. A. *J. Colloid Interface Sci.* **1992**, *153*, 188.
(19) Asher, S. A. U.S. Patents 4 627 689 and 4 632 517, 1986.
(20) Asher, S. A.; Flaugh, P. L.; Washinger, G. *Spectroscopy* **1986**, *1*, 26.
(21) Kesavamoorthy, R.; Super, M. S.; Asher, S. A. *J. Appl. Phys.* **1992**, *71*, 1116.
(22) Asher, S. A.; Kesavamoorthy, R.; Jagannathan, S.; Rundquist, P. In *SPIE Nonlinear Optics III*; Fisher, R. A., Reintjes, J. F., Eds.; International Society for Optical Engineering: Bellingham, WA, 1992; pp 238–242.
(23) Chang, T. Y. *Opt. Eng.* **1981**, *20*, 220.
(24) Rundquist, P. A.; Jagannathan, S.; Kesavamoorthy, R.; Brnardic, C.; Xu, S.; Asher, S. A. *J. Chem. Phys.* **1991**, *94*, 711.
(25) Rundquist, P. A.; Kesavamoorthy, R.; Jagannathan, S.; Asher, S. A. *J. Chem. Phys.* **1991**, *95*, 1249.
(26) Rundquist, P. A.; Kesavamoorthy, R.; Jagannathan, S.; Asher, S. A. *J. Chem. Phys.* **1991**, *95*, 8546.
(27) Sosnowski, S.; Feng, J.; Winnik, M. A. *J. Polym. Sci., Polym. Chem. Ed.* **1994**, *32*, 1497.
(28) Peterson, J. I. U.S. Patent 4 194 877, 1980.
(29) Loucif-Saïbi, R.; Nakatani, K.; Delaire, J. A.; Dumont, M.; Sekkat, Z. *Chem. Mater.* **1993**, *5*, 229.
(30) Brnardic, C. M.S. Thesis, University of Pittsburgh, 1992.
(31) Asher, S. A.; Holtz, J.; Liu, L.; Wu, Z. *J. Am. Chem. Soc.* **1994**, *116*, 4997.
(32) Gordon, P. F.; Gregory, P. *Organic Chemistry in Colour*; Springer-Verlag: Berlin, 1985.
(33) Vlyazlo, R. I.; Voloshin, G. A.; Grivnak, L. M.; Boldyrev, B. G.; Kozlov, L. V.; Zavalishchina, L. M. *Zh. Prikl. Khim. (Leningrad)* **1975**, *48*, 152.
(34) Haacke, G.; Panzer, H. P.; Magliocco, L. G.; Asher, S. A. U.S. Patent 5 266 238, 1993.
(35) Asher, S. A.; Jagannathan, S. U.S. Patent 5 281 370, 1994.
(36) Hiltner, P. A.; Papir, Y. S.; Krieger, I. M. *J. Phys. Chem.* **1971**, *75*, 1881.

MA950280G